# Tuning the Pressure-Induced Superconducting Phase in Doped $CeRhIn_5$

L. Mendonça Ferreira,[1] T. Park,[2,5] V. Sidorov,[2] M. Nicklas,[3] E. M. Bittar,[1] R. Lora-Serrano,[1] E. N. Hering,[4] S. M. Ramos,[4] M. B. Fontes,[4] E. Baggio-Saitovich,[4] Hanoh Lee,[2] J. L. Sarrao,[2] J. D. Thompson,[2] and P. G. Pagliuso[1]

[1]*Instituto de Física "Gleb Wataghin," UNICAMP, C.P. 6165, 13083-970, Campinas, Brazil*
[2]*Los Alamos National Laboratory, Los Alamos, New Mexico 87545, USA*
[3]*Max Planck Institute for Chemical Physics of Solids, Dresden D-01187, Germany*
[4]*Centro Brasileiro de Pesquisas Físicas, Rua Dr. Xavier Sigaud 150, 22290-180, Rio de Janeiro, Brazil*
[5]*Department of Physics, Sung Kyun Kwan University, Suwon 440-746, Korea*

(Received 7 March 2008; published 3 July 2008)

Pressure- and temperature-dependent heat capacity and electrical resistivity experiments on Sn- and La-doped $CeRhIn_5$ are reported for two samples with specific concentrations, $Ce_{0.90}La_{0.10}RhIn_5$ and $CeRhIn_{4.84}Sn_{0.16}$, which present the same $T_N = 2.8$ K. The obtained $P$-$T$ phase diagrams for doped $CeRhIn_5$ compared to that for the pure compound show that Sn doping shifts the diagram to lower pressures while La doping does exactly the opposite, indicating that the important energy scale to define the pressure range for superconductivity in $CeRhIn_5$ is the strength of the on-site Kondo coupling.

DOI: 10.1103/PhysRevLett.101.017005 PACS numbers: 74.70.Tx, 74.62.Fj, 75.30.Mb

The interplay between magnetism and superconductivity in strongly correlated electron systems has been intensively investigated in the past decades [1]. Particularly, the family of heavy fermion superconductors (HFSs) $CeMIn_5$ ($M$ = Rh, Co, Ir) (1-1-5) has allowed detailed investigation of this interplay in high-quality single crystals, where the antiferromagnetic (AFM) and the superconducting (SC) ground states can be found in their rich phase diagrams [2–8]. Among the (1-1-5)s, $CeRhIn_5$ is a particular member because its AFM ground state ($T_N = 3.8$ K) can be tuned to a SC phase by an external parameter such as pressure or doping [2,7,9]. In contrast, for the HFSs $CeCoIn_5$ [10] and $CeIrIn_5$ [11], long-range AFM order is established only by doping. For $CeRhIn_5$, specific heat measurements inside the SC state have shown that, in the range of pressures where $T_c > T_N$, the AFM became hidden and can be recovered by magnetic field [6]. This result suggests that the presence of superconductivity inhibits the intersite magnetic exchange interaction between the $4f$ electrons when $T_c > T_N$. Furthermore, NMR studies in Cd-doped $CeCoIn_5$ [12] has shown that Cd doping induces AFM droplets inside the SC phase by electronically tuning the Ce sites and suppressing SC locally. Thus, a competing relationship between AFM and SC appears to be a general trend for these compounds. However, microscopic coexistence of both states can be found in many regions of their phase diagrams [2,5,6,13]. Besides, it is evident from the studies above and others in $Ce_{1-x}La_xRhIn_5$ [14] and $CeRhIn_{5-x}Sn_x$ [15] that going farther way from the magnetic boundary also suppresses SC. This suggests that long-range AFM competes with the SC ground state but the magnetic fluctuations resulting from a suppressed magnetic state are important for SC. This statement, if proved right, may help shed light on the mechanisms of unconventional SC in the (1-1-5) materials and perhaps more broadly in other presumably magnetically mediated superconductors. In this regard, it is instructive to understand how different mechanisms for the suppression of long-range magnetism may affect the emergence of a magnetically mediated SC state.

$CeRhIn_5$ is a great material for studying how the pressure-induced SC phase is affected by a perturbation in the ambient pressure AFM state [6–9]. As such, in this work, we performed $P$-dependent experiments on single crystals of $Ce_{0.90}La_{0.10}RhIn_5$ and $CeRhIn_{4.84}Sn_{0.16}$. We have carefully chosen these two compositions because $T_N = 3.8$ K of the pure compound was suppressed to the same $T_N = 2.8$ K in both cases. For the La-doped sample, AFM is mainly suppressed by dilution, while increasing the Kondo coupling due to the introduction of an additional $p$ electron is the main mechanism for $T_N$ suppression in the Sn case [14–17].

It is known that, for $CeCoIn_5$, both La and Sn doping destroy the SC state, the latter being responsible for a more dramatic effect [16,18]. Therefore, the first expected effect on the $P$-induced SC state in our doped $CeRhIn_5$ would be a decrease of $T_c$. Second, as the AFM state is already partly suppressed by doping in both cases, one may anticipate that smaller $P$ would be required to drive $T_N$ to zero and induce SC.

In this Letter, we report two important results: (i) A pressure-induced SC phase was found for both La- and Sn-doped $CeRhIn_5$, and the doping-induced decrease in $T_c$ was found to be smaller than that for $CeCoIn_5$, and (ii) although the samples have the same $T_N$, Sn doping shifts the pressure phase diagram of $CeRhIn_5$ to lower pressures, while La doping does the opposite.

Single crystals of $Ce_{1-x}La_xRhIn_5$ and $CeRhIn_{5-x}Sn_x$ were grown from In flux and checked by x-ray diffraction (XRD). The $x$ was taken as the La/Ce ratio in the growth for the La-doped samples [14] and 40% of the Sn/In ratio in the growth for the Sn-doped crystals [15]. The lattice parameters and macroscopic properties obtained for the crystals used in this work were in agreement with previous

 

reports [14,15]. Measurements under hydrostatic pressure were carried out in a clamp-type cell. Pressure was determined by measuring $T_c$ for a Sn sample. ac resistivity was measured using the four contact configuration, and heat capacity was determined by the ac calorimetric technique [6].

Data from $T$-dependent electrical resistivity measurements for representative values of $P$ for $CeRhIn_{4.84}Sn_{0.16}$ and $Ce_{0.90}La_{0.10}RhIn_5$ are shown in Figs. 1 and 2, respectively. At ambient pressure, both samples show the characteristic behavior of the pure system [7,19]. At low $T$, $T_N$ is marked by a kink in the $\rho(T, P)$ data. No SC phase is found at ambient pressure down to the lowest $T$ achieved ($T \geq 0.3$ K). As was found for the pure compound [7,9], pressure induces, for both doped samples, a shift of the broad maximum centered at $T_{\max}$ initially to lower and then to higher $T$ as $P$ is increased.

Regarding the low-$T$ behavior, pressure-induced SC was found for both doped materials. For $CeRhIn_{4.84}Sn_{0.16}$, we first identify a down turn around 0.4 K in $\rho(T, P)$ for $P = 4$ kbar. A well-defined transition to a zero resistance state (ZRS) then emerges at $P = 8$ kbar and $T_c$ shifts to higher $T$ as pressure is increased. Similarly, a ZRS was also verified for $Ce_{0.90}La_{0.10}RhIn_5$ but only at higher pressure $P = 12$ kbar. The insets in Figs. 1 and 2 present the magnetic field-temperature phase diagram constructed from the $\rho(T, P)$ measurements. From the initial slope of the $H_{c2}(T)$ curves [20] at $P \approx 15$ kbar, we estimated the orbital $H_{c2}(0) = 80$ kOe and the coherence length $\xi = 60$ Å for $Ce_{0.90}La_{0.10}RhIn_5$ and $H_{c2}(0) = 70$ kOe and $\xi = 70$ Å for $CeRhIn_{4.84}Sn_{0.16}$.

Representative results for pressure-temperature-dependent heat capacity $C(T, P)$ measurements are displayed in Fig. 3. For pressures up to $P = 9.7$ kbar, a single anomaly at $T_N$ is seen for both samples. For the Sn-doped crystal, a broad peak initially emerges before a sharp anomaly is observed at lower $T$ and higher $P$. The temperature of this sharp anomaly and its $P$ and $H$ dependences (not shown) are consistent with the behavior of the ZRS, being, therefore, a signature of a bulk SC state. For the La-doped sample, only the sharp anomaly at $T_N$ is verified for all measured pressures. As we will discuss later, the $C(T, P)$ for the La-doped sample were not performed at high enough pressure to allow the observation of the SC heat capacity anomaly [21].

By mapping the $P$ evolution of the $T$ scales in our $\rho(T, P)$ data, we constructed the pressure-temperature ($P$-$T$) phase diagram shown in Fig. 4. Results for $CeRhIn_5$ [9] are included for comparison. For the two doped samples, $T_N$, $T_c$, and $T_{\max}$ follow the same qualitative evolution as a function of pressure found for pure $CeRhIn_5$ [see Fig. 4(a) and its inset] [7,9]. On the other hand, Fig. 4(b) presents the $T_N$ of the pure compound scaled to the same $T_N = 2.8$ K of the doped samples. Similarly, the maximum SC critical temperature $T_{c\,\max}$ achieved as a function of pressure for $CeRhIn_5$ and $Ce_{0.90}La_{0.10}RhIn_5$ was scaled to $T_{c\,\max} = 1.2$ K of the Sn-doped sample. Now, by comparing the $P$-$T$ phase diagram

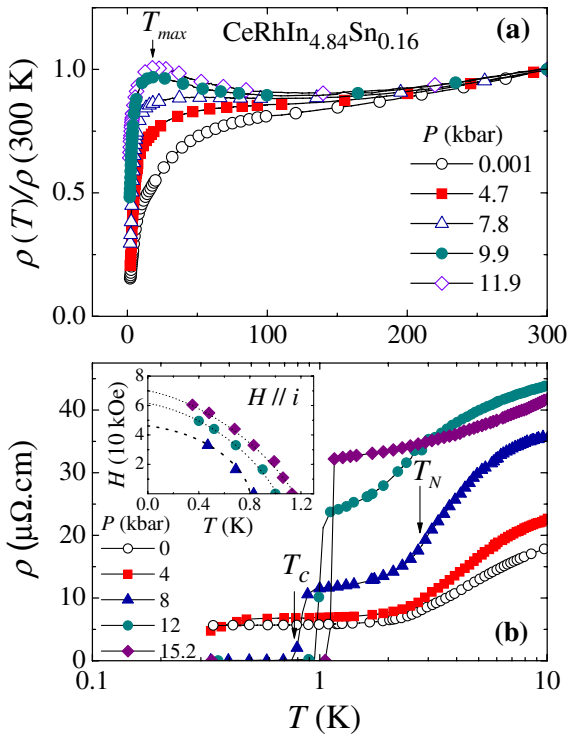


FIG. 1 (color online). (a) $\rho(T, P)$ for $CeRhIn_{4.84}Sn_{0.16}$ at selected pressures. (b) Low-$T$ data showing the signatures at $T_N$ and $T_c$. Inset: $H_{c2}(T)$ constructed from the $\rho(T, P, H)$ curves.

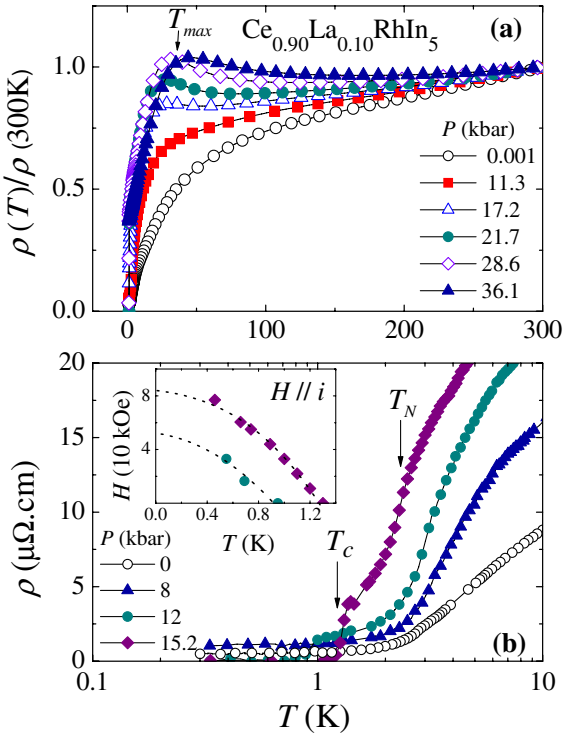


FIG. 2 (color online). (a) $\rho(T, P)$ for $Ce_{0.90}La_{0.10}RhIn_5$ for representative pressures. (b) Low-$T$ data showing the signatures at $T_N$ and $T_c$. Inset: $H_{c2}(T)$ constructed from $\rho(T, P, H)$.

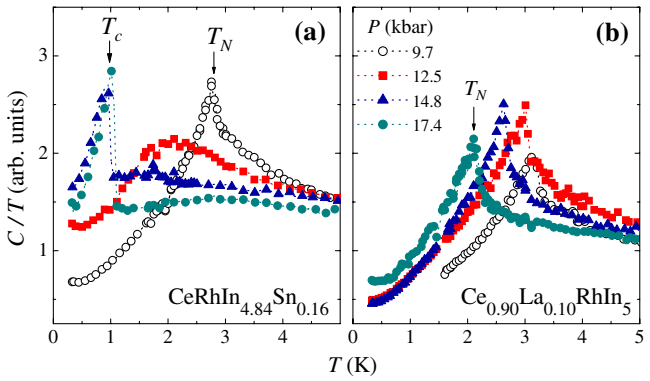


FIG. 3 (color online). $C(T)/T$ versus $T$ at different pressures for (a) $CeRhIn_{4.84}Sn_{0.16}$ and (b) $Ce_{0.90}La_{0.10}RhIn_5$.

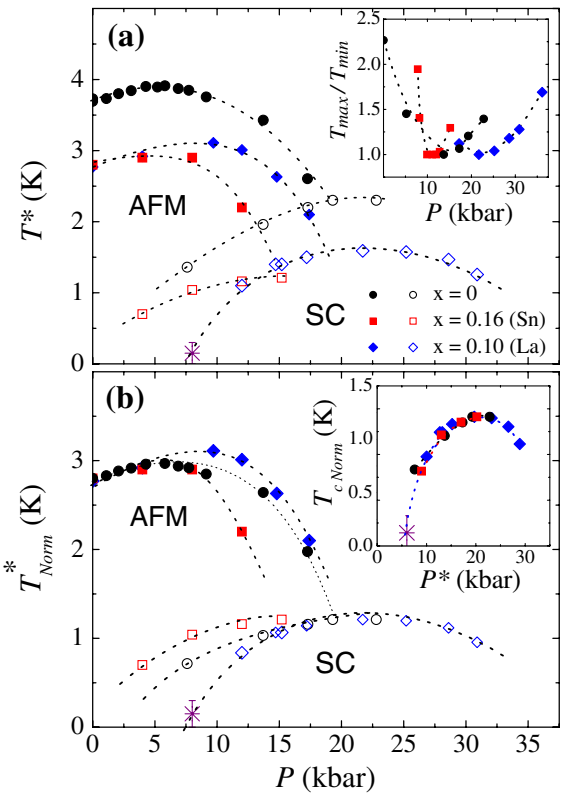


FIG. 4 (color online). (a) The $P$ dependence of the $T$ scales, extracted from the $\rho(P,T)$ for $CeRhIn_5$ (circles), $CeRhIn_{4.84}Sn_{0.16}$ (squares), and $Ce_{0.90}La_{0.10}RhIn_5$ (diamonds). Inset: $T_{max}$ normalized by their minimum values. (b) $T_N$ (solid symbols) and $T_c$ (open symbols) scaled to $T_N = 2.8$ K at ambient pressure and $T_{c\,max} = 1.2$ K, respectively. The star data point with an error bar at $P \approx 8$ kbar indicates that SC was not found down to 0.3 K only for $Ce_{0.90}La_{0.10}RhIn_5$. Results for $CeRhIn_5$ were extracted from Ref. [9]. Inset: $P$-$T$ phase diagram constructed using $P^* = P$, $P^* = P + 5.0$ kbar, and $P^* = P - 2.0$ kbar, for $CeRhIn_5$, $CeRhIn_{4.84}Sn_{0.16}$, and $Ce_{0.90}La_{0.10}RhIn_5$, respectively.

of the three samples on the same temperature scale [see Fig. 4(b)], one clearly sees that the La doping shifts the $P$-$T$ phase diagram of $CeRhIn_5$ to higher $P$ while the Sn doping does exactly the opposite.

As the two doped samples have the same $T_N$ at ambient pressure and similar strength of the Ce-Ce intersite magnetic coupling, our results suggest that it is the strength of the intrasite Kondo coupling which mainly determines the pressure evolution of the $CeRhIn_5$ ground state. As such, as La doping expands the lattice, it reduces the Kondo coupling and acts as a negative pressure. In contrast, Sn doping was found to increase the Kondo coupling by locally increasing the density of states at the Ce site [16], mimicking a positive pressure. One can use the measured lattice parameters of pure and 10% La-doped $CeRhIn_5$ [14] and the bulk modulus of the pure compound [22] to estimate the effective chemical pressure ($P_{chem}$) induced by La doping. Hence, using $-V_0 \partial P/\partial V \approx 780$ kbar, we calculated a $P_{chem} \approx -2.0$ kbar which is in fair agreement with the dome shift seen in Fig. 4(b). In the case of the Sn doping, no appreciable changes in the lattice parameters were found for this level of doping [15,17,23], but for both $CeRhIn_5$ and $CeCoIn_5$, it was found to increase the Kondo coupling and favor a localized to itinerant crossover of the Ce $4f$ electrons [15,16,23,24]. Therefore, as for other Ce compounds where $P$ also acts to enhance the Kondo coupling, the Sn doping clearly represents positive $P$. As $T_N$ and $T_{max}$ show a nontrivial evolution as a function of $P$ for $CeRhIn_5$, we used the monotonic pressure and Sn-doping dependences of $T_{max}$ for $CeCoIn_5$ to estimate the mimicked positive pressure ($P_{eff}$) induced by doping in $CeRhIn_{4.84}Sn_{0.16}$. Therefore, knowing $dT_{max}/dP$ ($\sim$3.0 K/kbar [25]) and $dT_{max}/d(\text{Sn-}x)$ ($\sim$6.0 K/at. % Sn [23] and $\sim$4.0 K/at. % Sn [17]) for $CeCoIn_5$, we estimate $P_{eff} = \sim 5$ kbar for our crystals of $CeRhIn_{4.84}Sn_{0.16}$, again in reasonable agreement with the SC dome shift seen in Fig. 4(b). The inset in Fig. 4(b) shows that the data of the three samples fall on top of each other when the pressure shifts discussed above are considered. Therefore, our data can be understood as a doping-induced tuning of the Kondo-coupling interaction of the Ce $4f$ electrons with the conduction band which is diminished by La doping and enhanced by Sn doping, despite both samples having the same $T_N$.

These results have an important consequence in the interplay between AFM and SC in these materials as they show that driving $T_N$ to zero does not necessarily favor the appearance of SC at the magnetic boundary. The suppression of the magnetism has to be associated with an increasing of $T_K$ and a consequent crossover between localized and itinerant behavior of the Ce $4f$, as observed by de Haas–van Alphen studies in $CeRhIn_5$ under pressure [26]. As such, if a given control parameter tunes $T_N$ to zero by a local mechanism, such as dilution or magnetic frustration which are not necessarily associated with an increase of the Kondo coupling, this tuning might in fact inhibit SC. For instance, SC is not found around the critical concentration ($x_c \approx 0.40$) in $Ce_{1-x}La_xRhIn_5$ [14]. Despite the disorder effects, according to our results, SC would be not expected at ambient pressure in this case, because the

La doping decreases the Kondo coupling, making the Ce $4f$ even more localized. Thus, SC could be found in this case only at much higher $P$ than pure $CeRhIn_5$. On the other hand, Sn doping shifts the pressure-induced SC phase of $CeRhIn_5$ to lower $P$. However, SC was not found at ambient pressure for $CeRhIn_{5-x}Sn_x$ [15]. Here, doping-induced disorder which gives rise to Abrikosov-Gorkov impurity scattering [16] has to be taken into account. Actually, the role of disorder is clear in the data reported here, since $T_{c\,\max}$ for the doped samples ($T_{c\,\max} = 1.2$ K for $CeRhIn_{4.84}Sn_{0.16}$ and $T_{c\,\max} = 1.6$ K for $Ce_{0.90}La_{0.10}RhIn_5$) is roughly a factor of 2 smaller than that for $CeRhIn_5$ ($T_{c\,\max} = 2.3$ K) [6]. However, it is interesting to note that the suppression of $T_{c\,\max}$ for $CeRhIn_{5-x}Sn_x$ (from 2.3 to 1.2 K for $x = 0.16$) and $Ce_{1-x}La_xRhIn_5$ (from 2.3 to 1.6 K for $x = 0.1$) are smaller than the suppression of the ambient pressure $T_c$ for $CeCoIn_{5-x}Sn_x$ (from 2.3 to 0.4 K for $x = 0.16$) [16,23] and $Ce_{1-x}La_xCoIn_5$ (from 2.3 to 1.2 K for $x = 0.1$) [18], respectively. These results suggest that impurity pair breaking may be enhanced for systems where the Ce $4f$ electrons become more hybridized with the conduction electrons. Interestingly, an earlier report [17] has found that applied pressure causes a decrease of $T_c$ in $CeCoIn_{5-x}Sn_x$ in contrast to the increase found for $CeCoIn_5$ in the same $P$ range. Furthermore, the residual resistivity at $T_c$ for the Sn-doped sample is larger than for the La-doped sample (see Figs. 1 and 2), even though the actual Sn concentration is smaller than in the La case.

The doping effects on the Kondo coupling may also explain our $C(T, P)$ data. The broad peak observed at $T \approx 2$ K for the Sn-doped crystal emerges at $P \approx 12$ kbar, before the sharp anomaly at $T_c$ sets in at $P = 14.8$ kbar (see Fig. 3). A similar broad feature was observed in the $C(T, H)$ data at ambient pressure for $Ce_{1-x}La_xRhIn_5$ at higher La-$x$ ($x \gtrsim 0.20$) as $T_N$ is suppressed [14,22]. This peak in $C(T)$ was successfully interpreted in terms of short-range magnetic order using a 2D-Ising model [22]. Here, in the case of $CeRhIn_{4.84}Sn_{0.16}$, for the pressure range where the broad peak appears, the sample presents already a ZRS at lower $T$ (see Figs. 1 and 3). We believe that the above results can be understood in a similar way as for the Cd-doping-induced AFM droplets in $CeCoIn_{5-x}Cd_x$. When Sn replaces In, it increases $T_K$ locally, tending to suppress the AFM correlations in the vicinity of the Sn dopant, allowing SC droplets to form locally. When SC droplets form a filamentary shortcut, they give rise to a ZRS state. As AFM is locally suppressed on several sites, the long-range AFM disappears, leaving a remaining short-ranged AFM phase that still occupies most of the sample volume, which generates the broad peak in $C(T, P)$. As pressure is increased, the hybridization strength is increased on all sites, and the SC becomes a bulk state. NMR studies in $CeRhIn_{5-x}Sn_x$ as a function of pressure would be valuable to confirm the above speculation.

For the La-doped sample, the AFM at $T_N$ can be seen in the $C(T, P)$ up to the highest $P$ applied. In this case, as the La-doping-induced lattice expansion is a more bulky effect as observable by XRD, most of the Ce $4f$ spins remain localized up to a higher value of pressure, and therefore the long-range AFM signature can persist at higher $P$. As SC droplets may develop as a function of pressure in sites farther from the La impurities, a ZRS can be achieved as a SC path is formed, but bulk SC would appear only for higher $P$.

In summary, we present $\rho(T, P)$ and $C(T, P)$ data for La-doped and Sn-doped $CeRhIn_5$. As for the pure compound, a $P$-induced SC state is found for both samples. However, by comparing their $P$-$T$ phase diagrams to that of $CeRhIn_5$, we found that, although the two doped samples have the same $T_N$, they shift the $P$-$T$ phase diagram of the pure compound in opposite directions, revealing that the strength of the Kondo coupling is the relevant energy scale to set the pressure range for occurrence of SC in $CeRhIn_5$.

The authors thank Fapesp-SP, CNPq (Brazil), and U.S. DOE for financial support.

[1] M. A. Continentino, Braz. J. Phys. **35**, 197 (2005).
[2] P. G. Pagliuso *et al.*, Phys. Rev. B **64**, 100503(R) (2001).
[3] P. G. Pagliuso *et al.*, Physica (Amsterdam) **312B–313B**, 129 (2002).
[4] L. D. Pham *et al.*, Phys. Rev. Lett. **97**, 056404 (2006).
[5] V. S. Zapf *et al.*, Phys. Rev. B **65**, 014506 (2001).
[6] T. Park *et al.*, Nature (London) **440**, 65 (2006).
[7] H. Hegger *et al.*, Phys. Rev. Lett. **84**, 4986 (2000).
[8] T. Mito *et al.*, Phys. Rev. B **63**, 220507(R) (2001).
[9] M. Nicklas *et al.*, Phys. Rev. B **70**, 020505(R) (2004).
[10] C. Petrovic *et al.*, J. Phys. Condens. Matter **13**, L337 (2001).
[11] C. Petrovic *et al.*, Europhys. Lett. **53**, 354 (2001).
[12] R. R. Urbano *et al.*, Phys. Rev. Lett. **99**, 146402 (2007).
[13] Guo-qing Zheng *et al.*, Phys. Rev. B **70**, 014511 (2004).
[14] P. G. Pagliuso *et al.*, Phys. Rev. B **66**, 054433 (2002).
[15] E. D. Bauer *et al.*, Physica (Amsterdam) **378B–380B**, 142 (2006).
[16] M. Daniel *et al.*, Phys. Rev. Lett. **95**, 016406 (2005).
[17] S. M. Ramos *et al.*, Physica (Amsterdam) **359B–361B**, 398 (2005); S. M. Ramos, Ph.D. thesis, UFF, Brazil, 2007.
[18] C. Petrovic *et al.*, Phys. Rev. B **66**, 054534 (2002).
[19] A. D. Christianson *et al.*, Phys. Rev. B **66**, 054410 (2002).
[20] N. R. Werthamer *et al.*, Phys. Rev. **147**, 295 (1966).
[21] A resistive transition is also found in the absence of a specific heat feature even in undoped $CeRhIn_5$ when $T_N > T_c$ (see Ref. [6]).
[22] Ravhi S. Kumar *et al.*, Phys. Rev. B **69**, 014515 (2004).
[23] E. D. Bauer *et al.*, Phys. Rev. B **73**, 245109 (2006).
[24] J. G. Donath *et al.*, Physica (Amsterdam) **460C–462C**, 661 (2007).
[25] M. Nicklas *et al.*, J. Phys. Condens. Matter **13**, L905 (2001).
[26] H. Shishido *et al.*, J. Phys. Soc. Jpn. **74**, 1103 (2005).